



# Influence of nickel precipitation on the formation of denuded zone in Czochralski silicon

Jin Xu<sup>a,b,\*</sup>, Yongzhi Wang<sup>a</sup>, Deren Yang<sup>b</sup>, H.J. Moeller<sup>c</sup>

<sup>a</sup> Department of Materials Science and Engineering, College of Materials, Xiamen University, Xiamen, Fujian 361005, People's Republic of China

<sup>b</sup> State Key Laboratory of Silicon Materials, Zhejiang University, Hangzhou 310027, People's Republic of China

<sup>c</sup> Institute for Experimental Physics, TU-Freiberg, SilbermannStr. 1, 09596 Freiberg, Germany

## ARTICLE INFO

### Article history:

Received 4 March 2010

Received in revised form 16 April 2010

Accepted 23 April 2010

Available online 5 May 2010

### Keywords:

Denuded zone

RTA annealing

Czochralski silicon

Nickel

## ABSTRACT

The influence of nickel precipitation on the formation of denuded zone (DZ) in Czochralski silicon (Cz Si) was systematically investigated by means of Scanning Infrared Microscopy (SIRM) and optical microscopy (OM). It was found that, for conventional high-low-high annealing (CFA), the DZ can be obtained in all specimens contaminated by nickel impurity at different steps of the heat treatment, indicating that no nickel precipitates generated in the region just below the surface. Additionally, the width of the DZ is nearly the same in all specimens although the contamination sequence is different, indicating that the contamination temperature, that is, the corresponding equilibrium concentration of interstitial nickel in the silicon doesn't influence significantly the thermodynamics and kinetics process of the formation of nickel precipitates. For Rapid thermal annealing (RTA)-low-high annealing, the tendency remained unchanged. On the basis of the experimental results, it is supposed that the formation of DZ is strongly influenced by the segregation gettering and intrinsic gettering of the nickel atoms, which were caused by the formation of nickel-silicon (Ni-Si) alloys close to the surface, oxygen precipitates and extended defects in the bulk, respectively.

© 2010 Elsevier B.V. All rights reserved.

## 1. Introduction

In modern integrated circuit (IC) device processes, the defect-free zones close to Cz Si wafer surface becomes increasingly important for device yield. It has been well accepted that transition metals, particularly nickel, iron and copper, are extremely detrimental to the performance of IC devices due to their high diffusivity and solubility at elevated temperature and the formation of electrical levels in the band gap and precipitates in p–n junctions. Thus, the removal of the transition metals by the oxygen precipitates and related defects, back-side damage, phosphorous diffusion and implantation-induced damage, etc., from device active regions has proven indispensable to improve the yield of IC devices. It is well recognized that 3d-transition metals precipitation process is strongly dependent on the doping type and concentration, cooling rates, intrinsic point defects and induced defects in bulk silicon [1–5]. Recently, nickel gettering has been paid more attention because nickel contamination degrade the gate oxide integrity, which is comparable to the breakdown effects due to iron contam-

ination [3]. Nickel, as one of the most important transition metals, easily contaminates silicon wafers and device from stain-less steel equipments due to its rapid diffusion. The existence of nickel impurity is deleterious to the device performance either by forming silicides or by acting as recombination centers, thus it makes the subject of effective gettering of nickel extremely important and has attracted much attention in the past decades [4–7]. In general, nickel primarily exists in interstitial site and the solubility of interstitial nickel decrease sharply with the decrease of temperature, thus, the nickel precipitation is easily to occur during cooling. Nickel precipitates can influence the electrical property of devices due to the introduction of energy levels in band gap [6,8–13].

It was reported that various kinds of Ni–Si alloy formed on the surface during the in-diffusion heat treatment of nickel in silicon wafers. Considering the difference of nickel solubility between silicon and Ni–Si alloy, Gay deduced that in the defect-free silicon, the behavior of nickel was mainly controlled by the segregation gettering, namely the nickel atoms is prefer to be absorbed by the Ni–Si alloy formed on the surface due to its stronger gettering ability [14–16]. On the other hand, oxygen is inevitably incorporated into the silicon directly from the quartz crucibles during Cz Si growth process [1,17,18]. Considering the oxygen is incorporated at about 1400 °C, it is easy to understand that the interstitial oxygen is supersaturated in silicon bulk at temperature characteristic of device processing, generally lower than 1200 °C. During the

\* Corresponding author at: Department of Materials Science and Engineering, College of Materials, Xiamen University, Xiamen, Fujian 361005, People's Republic of China. Tel.: +86 592 2180 775; fax: +86 592 2183 937.

E-mail addresses: [xujinmse@xmu.edu.cn](mailto:xujinmse@xmu.edu.cn) (J. Xu), [mseyang@zju.edu.cn](mailto:mseyang@zju.edu.cn) (D. Yang).

**Table 1**  
Annealing sequence and nickel contamination process.

Specimens	Annealing sequence			
	I	II	III	IV
A1	1150 °C/4 h	750 °C/8 h	Ni contamination	1050 °C/16 h
M1	1250 °C/60 s	750 °C/8 h	Ni contamination	1050 °C/16 h
A2	1150 °C/4 h	Ni contamination	750 °C/8 h	1050 °C/16 h
M2	1250 °C/60 s	Ni contamination	750 °C/8 h	1050 °C/16 h
A3	Ni contamination	1150 °C/4 h	750 °C/8 h	1050 °C/16 h
M3	Ni contamination	1250 °C/60 s	750 °C/8 h	1050 °C/16 h

subsequent processes of devices fabrication, supersaturated oxygen atoms will agglomerate to form precipitates and furthermore to induce dislocation and stacking fault, acting as effective gettering sites for impurities. Conventionally, on the basis of the oxygen out-diffusion and oxygen precipitation mechanism, DZ can be created by high-low-high heat treatments. Obviously, the formation of DZ is sensitive to initial oxygen concentration, thermal history and carbon concentration, etc. [19–21]. Recently, RTA technology was employed to build a vacancy concentration depth profile in silicon wafer, which is another approach for the creation of DZ. Followed by low-high two-step annealing, the oxygen precipitation behavior is well controlled by vacancy profile rather than oxygen concentration profile, thus DZ is believed to be independent of the initial oxygen concentration, thermal history and so on [22,23].

As mentioned above, no matter from the academic view or industrial objective, it is important to study the nickel precipitation mechanism during the DZ formation process in order to form an effective IG structure consisting of an ideal BMD density and distribution, and defect-free zones. However, few papers to date have been published about the influence of nickel precipitation on the formation of DZ investigated by SIRM according to the author's knowledge. In this article, the SIRM and OM were used to reveal the distribution of nickel precipitate colonies generated during the DZ formation annealing. SIRM is a powerful tool to investigate oxygen and metal precipitates in silicon due to its convenient and nondestructive feature [24,25]. The local stress introduced in silicon matrix by the nickel precipitate colonies formed during cooling can produce contrast, which can be detected by SIRM. In the experiments, it was found that, for both CFA and RTA-low-high annealing process, no nickel precipitation occurred in the region just below the surface in all specimens contaminated by nickel impurity at different steps. The interaction among the Ni-Si alloy formed on the surface, oxygen precipitates and extended defects in the bulk, and the nickel impurity was used to explain the mechanism of nickel precipitation in Czochralski silicon.

## 2. Experimental details

The specimens used in this experiment were cut from P-type, (1 0 0)-orientation, 8 in. Cz Si ingot grown in argon atmosphere. The specimens were cut into 2 cm × 2 cm pieces, and then chemically polished with CP4, cleaned with the standard RCA (SC-1 and SC-2) process, and finally etched with 5% HF solution to remove surface native oxide. The carbon and oxygen concentrations were determined by a Nicolet 410 Fourier transform infrared spectrometer (FTIR) at room temperature. The initial concentration of interstitial oxygen ( $1107\text{ cm}^{-1}$ ) is about  $8.5 \times 10^{17}\text{ cm}^{-3}$  with the calibration factor of  $3.14 \times 10^{17}\text{ cm}^{-2}$ , and that of substitutional carbon ( $605\text{ cm}^{-1}$ ) below the detection limit of FTIR. Prior to the CFA and RTA-low-high annealing, the specimens were divided into three groups, numbered A1, A2, A3 and M1, M2, M3, respectively. The specimens were immersed in  $\text{Ni}(\text{NO}_3)_2 \cdot 6\text{H}_2\text{O}$  solution for 4 min to introduce intentionally nickel contamination on the sample surface. The nickel concentration is 0.5 mol/l, which is much higher than the nickel saturation concentration of about  $10^{18}\text{ atoms/cm}^3$  in silicon at 1100 °C. The in-diffusion of nickel impurity into the silicon bulk was realized by thermal drive-in annealing performed at different temperature. The detailed annealing sequence and nickel contamination process are listed in Table 1. After each step annealing, the samples were usually taken out of the furnace to cool in air with a cooling rate of about 30 K/s.

After cooling, each specimen was cut into two parts and fixed them face to face by epoxy resin. Then, a slow speed diamond saw was used to cut the specimens along the direction perpendicular to the surface. The cross section structures were scanned by SIRM with a detection limit of about 60 nm, following chemically and mechanically polishing. After the SIRM investigation, the specimens were cleaved and etched in Sirtl etchant for 4 min. Finally, OM was applied to observe the cross section of the specimens to determine the density and distribution profile of BMDs, which is related to the oxygen precipitates, nickel precipitates and induced defects.

## 3. Results and discussion

### 3.1. Contamination after the second low temperature annealing

In this section, the samples A1 and M1 were firstly treated by CFA at 1150 °C for 4 h and by RTA at 1250 °C for 60 s, respectively, followed by annealing at 750 °C for 8 h. The Ni impurity was introduced into the silicon wafer by immersing the samples into the  $\text{Ni}(\text{NO}_3)_2 \cdot 6\text{H}_2\text{O}$  solution, then the samples with  $\text{Ni}(\text{NO}_3)_2 \cdot 6\text{H}_2\text{O}$  solution were sent into a quartz furnace, annealed at 1050 °C for 16 h. Considering the high diffusivity, the nickel impurity reach its saturation concentration in whole silicon bulk during the in-

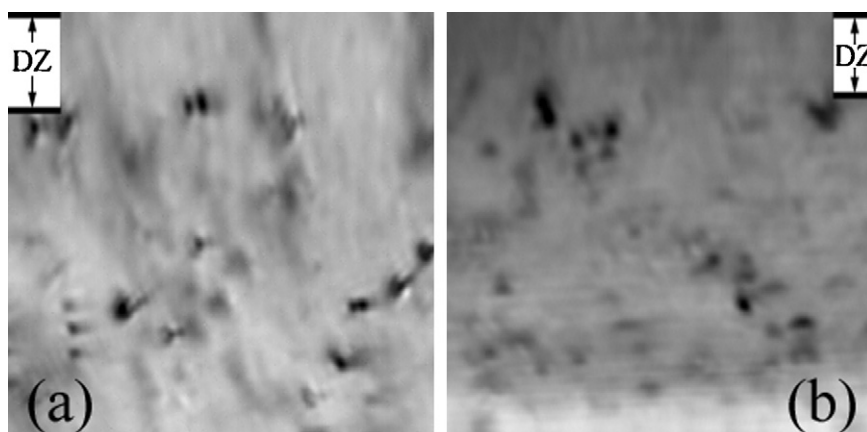


**Fig. 1.** SIRM images of the BMDs in the sample contaminated by nickel after the second low temperature annealing: A1 (a) and M1 (b). Image size: 100  $\mu\text{m}$  × 100  $\mu\text{m}$ .

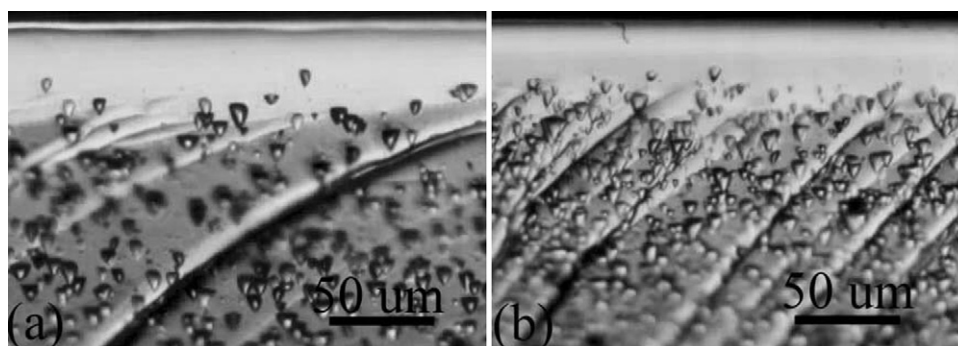


Fig. 2. OM images of the BMDs distribution in the sample contaminated by nickel after the second low temperature annealing: A1 (a) and M1 (b).

diffusion annealing. Fig. 1 shows the density and distribution of BMDs observed from the direction perpendicular to the cross section by SIRM, verifying the formation of DZ in both samples. It can be seen from Fig. 1 that the nickel precipitate colonies are of large contrast, indicating that the local stress generated in the silicon matrix is huge due to the large lattice misfit between nickel silicide precipitates and silicon matrix, while some precipitates display weak contrast because they were out of the light focus.

It is generally believed that nickel silicides have a size distribution, obviously, smaller precipitates with size less than 60 nm cannot be detected by SIRM and the density value given above is probably underestimated. Therefore, to further confirm if there are smaller precipitates (<60 nm) generated in the zone close to the surface, OM combined with etching was used to observe the BMD distribution along the cross section. As shown in Fig. 2, a high density of BMDs was found to exist in the bulk, while no BMDs generated in the zone just below the surface in both samples, further manifested the formation of DZ in A1 and M1 specimens. The width of the DZ in A1 specimens is about 25  $\mu\text{m}$  and 20  $\mu\text{m}$  in M1 specimen, respectively, which is consistent with the SIRM results. It was revealed that the density of BMDs in the bulk was estimated to be about  $5 \times 10^7 \text{ cm}^{-3}$  in the CFA sample (Fig. 2(a)) and  $10^8 \text{ cm}^{-3}$  in the RTA-low-high sample (Fig. 2(b)), respectively. The reason is related to the enhancement of oxygen precipitation by vacancy injected into the silicon bulk during 1250  $^{\circ}\text{C}/60 \text{ s}$  RTA annealing.

### 3.2. Contamination after the first high temperature annealing

In this section, the samples A2 and M2 were firstly treated by CFA at 1150  $^{\circ}\text{C}$  for 4 h and by RTA at 1250  $^{\circ}\text{C}$  for 60 s, respectively, and then dipped into  $\text{Ni}(\text{NO}_3)_2 \cdot 6\text{H}_2\text{O}$  solution, followed by 750  $^{\circ}\text{C}/8 \text{ h} + 1050 \text{ }^{\circ}\text{C}/16 \text{ h}$  annealing. According to the SIRM investigation of the BMD distribution along the cross section, the formation of DZ in both specimens is nearly the same as that discussed in sec. III A. Again, OM was used to observe the BMDs distribution along the cross section. The density of the BMDs in the bulk was also about  $5 \times 10^7 \text{ cm}^{-3}$  and  $10^8 \text{ cm}^{-3}$ , respectively, while in the zone just below the surface is nearly zero. The DZ width in the two samples is also about 25  $\mu\text{m}$  and 20  $\mu\text{m}$ , respectively.

### 3.3. Contamination before the first high temperature annealing

After the Ni contamination, the samples A3 and M3 were put into furnaces, then annealed at 1150  $^{\circ}\text{C}$  for 4 h by CFA or treated at 1250  $^{\circ}\text{C}$  for 60 s by RTA, respectively, followed by 750  $^{\circ}\text{C}/8 \text{ h} + 1050 \text{ }^{\circ}\text{C}/16 \text{ h}$  annealing. In the two samples, the DZ with the width of about 25  $\mu\text{m}$  and 20  $\mu\text{m}$  in the near surface, respectively, and BMDs with high density in the bulk were observed by both of SIRM and OM, which is similar to the results described in the sec. III A.

Due to the sharp dependence of the solubility on temperature, the interstitial nickel atoms, which can diffuse into silicon wafers at high temperature, tended to agglomerate and form nickel silicide during the subsequent air cooling, the reaction is presented as follows [4,6,8,15]:



It has been well accepted that during nickel precipitation, the equilibrium phase is  $\text{NiSi}_2$ , which has the cubic structure of fluoride  $\text{CaF}_2$ . It was reported that the lattice parameter of  $\text{NiSi}_2$  is less than that of silicon by 0.4% (0.5406 nm compared with 0.5428 nm), thus the volume change associated with nickel precipitation is small. Compared with the formation of copper silicide in silicon, it is reasonable to deduce that the stress generated around the  $\text{NiSi}_2$  will not impose significant influence on the nickel precipitation [4,15,26].

Transition metals are well known to be fast diffusers. The diffusion coefficient of nickel is strongly dependent on the temperature, which is  $10^{-5} \text{ cm}^2/\text{s}$  at 750  $^{\circ}\text{C}$  and  $10^{-4} \text{ cm}^2/\text{s}$  at 1250  $^{\circ}\text{C}$  according to the theoretical calculation and extrapolation, respectively [4,24,25]. In view of the annealing time and temperature used in the experiments, it can be inferred that the diffusion length of nickel impurity is many times longer than the thickness of the silicon samples, thus, the  $\text{Ni}_i$  can soon reach its saturation concentration and distribute uniformly in the whole wafer.

It has been well established that the precipitation process of transition metals in Cz Si has been controlled by two parameters, one is the driving force related with the supersaturation of transition metals, the other is the barrier imposed by phase transformations. Compared with the Cu precipitation, the local stress generated in the silicon matrix is negligible due to the small lattice misfit between nickel silicide and silicon matrix. It was reported that there are two preferred reaction paths of the supersaturated transition metals in Cz Si after in-diffusion and cooling down, either precipitation in the bulk or diffuse to its surface [8,14,15,26]. Considering the high diffusivity, for the samples A1 and M1, it can be concluded that the  $\text{Ni}_i$  was introduced into the silicon bulk and reach its saturation concentration after the in-diffusion annealing at 1050  $^{\circ}\text{C}$  for 16 h. During the cooling in air with a cooling rate of about 30 K/s, the supersaturation level of  $\text{Ni}_i$  builds up rapidly, leading to the significant increase of driving force. As a consequence, the nickel precipitation is easily occurred, either in the bulk or on the surface according to the discussion mentioned above.

As mentioned above, the supersaturated oxygen atoms can form oxygen precipitates which act as effective gettering sites for transition metals in the bulk of Cz silicon wafer [1,7,14]. As for the A1 and M1 specimens, the oxygen precipitate nuclei with high density generated during the annealing at 750  $^{\circ}\text{C}$  for 8 h, serving as the preferred sites for the precipitation of the Ni silicide. Thus, it is

rational to deduce that during the subsequent cooling from 1050 °C annealing, part of the supersaturated nickel atoms diffused to the existing oxygen precipitates intentionally formed in the regions away from the device surface and be absorbed. On the contrary, the oxygen out-diffusion curve or vacancy depth profile formed after annealing at 1150 °C for 4 h or by RTA, at 1250 °C for 60 s, respectively, make the surface region deplete of oxygen precipitates. On the other hand, it was reported that the temperature at the surface decreased more quickly than that in the bulk during cooling, resulting in larger driving force than that in the bulk, leading to the formation of Ni–Si alloy on the surface [14,15,25]. Considering the difference of nickel solubility between silicon and Ni–Si alloy, it is obvious that the region of higher solubility acts as a sink for transition metals from the lower solubility region, leading to the gettering of another part of nickel atoms by the Ni–Si alloys on the surface. Combining with the analysis mentioned above, it is reasonable to deduce that nickel atoms preferred to be absorbed by Ni–Si alloy and oxygen precipitates rather than deposited in the region below the surface, leading to the formation of DZ.

For sample A2 and M2, the oxygen out-diffusion curve or vacancy depth profile formed after annealing at 1150 °C for 4 h or by RTA, at 1250 °C for 60 s, respectively [19,22]. It has been widely accepted the nickel precipitation temperature in Cz silicon is above 800 °C, and nickel mainly occupied interstitial sites or formed different types of nickel complexes if the annealing temperature was lower than 800 °C, such as 750 °C [14,15,25]. For the interstitial oxygen atoms in Cz Si, it is well known that 750 °C is the optimum temperature for oxide precipitates to nucleate [1,2,26], which hints that the oxygen precipitate nuclei can act as the sink to absorb part of Ni<sub>i</sub> due to the lower barrier. It should be pointed out here that the oxygen precipitate nuclei only exist in the bulk while not in the region just below the surface. Consequently, it is reasonable to come up with a hypothesis that in the samples A2 and M2, the Ni impurity introduced into the bulk of a wafer during 750 °C thermal drive-in annealing will not form precipitates in the region close to the surface, but diffuse back to the surface or trapped by the oxygen precipitate nuclei after the wafer is taken out of the furnace. Finally, oxygen precipitate with high density and induced extended defects generated in the bulk of the samples underwent the annealing at 1050 °C for 16 h, which is sufficient for the effective trapping of nickel impurity. By taking into account the loss of nickel impurity due to the diffusion to the surface and absorption by oxygen precipitates nuclei, which is the IG process, it can be easily understood that although the temperature here, 1050 °C, higher than the precipitation temperature, 800 °C, the amount of the nickel impurity which can diffuse to the zone just below the surface and form nickel precipitate colonies is negligible, leading to the formation of DZ.

In sample A3 and M3, denuded zone also formed in both samples. The main reason has been ascribed to the Ni–Si alloy formed on the surface during the first high temperature annealing, 1150 °C for 4 h or by RTA, at 1250 °C for 60 s, respectively. Here, the self-gettering process plays an important role on the gettering of transition metals impurity atoms which have diffused into the bulk of the silicon. During the cooling process, the surface was still coated with the nickel contaminants, which would have reacted with the silicon to form Ni–Si alloy. As mentioned above, the solubility of nickel impurity in the Ni–Si alloy is higher than that in silicon, thus the supersaturated Ni<sub>i</sub> diffused back to the surface and trapped by Ni–Si alloy [4,7,14,26]. During the 750 °C/8 h + 1050 °C/16 h annealing, the Ni–Si alloy will not dissolve due to the complexity of the dissolution process, make the bulk of silicon wafer deplete of the nickel impurity. In other words, even though there are some mobile nickel impurities existed in the silicon bulk due to the dissolution of nickel precipitates, it can be

trapped by the nuclei and extended defects, respectively, generated during the 750 °C and 1050 °C annealing, the same as what happened in samples A2 and M2. According to the analysis mentioned above, it can be concluded that the no nickel precipitate colonies formed, both in the zone just below the surface and bulk.

It should be emphasized that in all samples the last thermal treatment was carried out at 1050 °C for 16 h, which will lead to the dissolution of nickel precipitates inevitably. It was reported [6,27–31] that the transition metals silicide precipitates can be dissolved into the silicon substrate during subsequent high temperature annealing, here is 1050 °C. It is easy for nickel silicides to dissolve from the structural defect due to the high solubilities and diffusivities of nickel [28]. As mentioned above, the supersaturated interstitial nickel impurities can diffuse to the surface or precipitate in the bulk [14–17,32,33]. Considering the analysis discussed above, it is reasonable to deduce that the supersaturated nickel atoms can be trapped by the existing oxygen precipitates and Ni–Si alloy formed on the surface, respectively.

It was revealed that the width of the DZ is nearly the same for samples A1–A3, and M1–M3, respectively, while the width of M1–M3 is narrower than that of the samples A1–A3. The main reason has been ascribed to the formation of Ni–Si alloy and the oxygen out-diffusion curve or vacancy depth profile created during the first high temperature annealing. Considering the equilibrium concentration of nickel impurity, which is the highest in samples A3 and M3 because of the highest introduction temperature. In view of the sharp dependence of the solubility of interstitial nickel on temperature, it is obvious that the Ni<sub>i</sub> concentration introduced into sample A3 and M3 is about two orders of magnitude higher than that of sample A2 and M2. On the other hand, the Ni–Si alloy formed on the surface has a strong ability to absorb the nickel atoms due to its higher solubility. In addition, it was reported [34] that the threshold of oxygen precipitates for the complete gettering of nickel is about  $3 \times 10^6 \text{ cm}^{-3}$ , less than that revealed in our paper. Obviously, the oxygen precipitates exhibited a huge potential for the gettering of nickel impurity. In view of the above discussions, it can be concluded that under the coaction of these two elements given above, the DZ width was determined by the oxygen out-diffusion curve or vacancy depth profile, while, it was independent of the nickel contamination sequence, namely, the corresponding equilibrium concentration of interstitial nickel in silicon. As for the BMDs density of samples M1–M3, which was relatively higher in comparison with that of samples A1–A3. It was believed that the difference was mainly caused by the enhancement effect of vacancies on oxygen precipitation [22,35]. The RTA-induced vacancies can significantly facilitate the formation of oxygen precipitate nuclei during the 750 °C annealing and, moreover, enhance oxygen precipitation during the subsequent 1050 °C annealing.

In our paper, the distribution of BMDs along the cross section was investigated by SIRM and OM in all the samples, which can be explained satisfactorily by the discussions mentioned above. The difference in the BMDs density was explained in terms of the vacancy generated by the RTA annealing. Another prominent feature of the nickel precipitation is that, compared with that of copper precipitation, the barrier imposed by phase transformations is negligible. Considering the small lattice misfit and the corresponding stress, it should be pointed out that the influence of the point defects on the generation of nickel silicides is not significant [4,15,26,36]. In view of the analysis given above, it is reliable to deduce that the RTA-induced vacancies will not influence the behavior of nickel impurity to a large extent, which is consistent with the formation mechanism of DZ mentioned above. To elucidate the formation of DZ in A1 and M1 specimens, an explanation was proposed taking into account both intrinsic gettering and external gettering of metals at oxygen clusters and surface sites, respectively.

#### 4. Conclusion

In this paper, the influence of nickel precipitation on the formation of denuded zone was systematically investigated by SIRM and OM. It was revealed that the DZ can be obtained in all samples contaminated by nickel impurity. Furthermore, the width of the DZ is nearly the same in A1–A3 and M1–M3 specimens, respectively, indicating that the DZ formation was controlled by oxygen out-diffusion curve or vacancy depth profile, while independent of the nickel contamination sequence. Considering the small lattice misfit and the corresponding stress, it can be concluded that the influence of the point defects on the generation of nickel silicides is not significant. The enhancement of oxygen precipitation was caused by the vacancies, which injected into the silicon bulk during 1250 °C/60 s RTA annealing. On the basis of the experimental results, it can be derived that the segregation gettering and intrinsic gettering of the nickel atoms plays an important role on the formation of DZ, where no nickel silicides and oxygen precipitates existed.

#### Acknowledgments

The work was partly supported by Program for New Century Excellent Talents in Fujian Province University and Nation Natural Science Foundation of China (No. 50902116 and No. 50832006). The work was also partly supported by the Opening Project of State Key Laboratory of Silicon Materials (No. SKL2009-11). The authors would also like to thanks E. Kubsch for her kindly help.

#### References

- [1] A. Borghesi, B. Pivac, A. Sassella, A. Stella, *J. Appl. Phys.* 77 (1995) 4196.
- [2] G.A. Rozgonyi, R.P. Doysher, C.W. Pearce, *J. Electrochem. Soc.* 123 (1910) 1976.
- [3] R. Hoelzl, K.-J. Range, L. Fabry, J. Hage, V. Raineri, *Mater. Sci. Eng. B* 73 (2000) 95.
- [4] E.R. Weber, *Appl. Phys. A* 30 (1983) 1.
- [5] B. Bokhonov, M. Korchagin, *J. Alloys Compd.* 319 (2001) 187.
- [6] S.M. Myers, M. Seibt, W. Schroeter, *J. Appl. Phys.* 88 (2000) 3795.
- [7] S.A. Mchugo, H. Hieslmair, E.R. Weber, *Appl. Phys. A* 64 (1997) 127.
- [8] A.A. Istratova, E.R. Weber, *Appl. Phys. A* 66 (1998) 123.
- [9] M. Seibt, H. Hedemann, A.A. Istratov, F. Riedel, A. Sattler, W. Schröter, *Phys. Status. Solidi A* 171 (1999) 301.
- [10] B. Shen, R. Zhang, Y. Shi, Y.D. Zheng, T. Sekiguchi, K. Sumino, *Appl. Phys. Lett.* 68 (1996) 214.
- [11] R. Rizk, X. Portier, G. Allais, G. Nouet, *J. Appl. Phys.* 76 (1994) 952.
- [12] O. Palais, E. Yakimov, S. Martinuzzi, *Mater. Sci. Eng. B* 91 (2002) 216.
- [13] Hideki Takahashi, Masashi Suezawa, Koji Sumino, *Jpn. J. Appl. Phys.* 36 (1997) 6807.
- [14] N. Gay, S. Martinuzzi, *Appl. Phys. Lett.* 70 (1997) 2568.
- [15] Z.Q. Xi, D.R. Yang, J. Chen, D.L. Que, H.J. Moeller, *Physica B* 344 (2004) 407.
- [16] Z. Rao, J.S. Williams, A.P. Pogany, D.K. Sood, G.A. Collins, *J. Appl. Phys.* 77 (1995) 3782.
- [17] T.Y. Tan, E.E. Gardner, W.K. Tice, *Appl. Phys. Lett.* 30 (1977) 175.
- [18] D. Cavalcoli, A. Castaldini, A. Cavallini, *Appl. Phys. A* 90 (2008) 619.
- [19] Z.Q. Xi, J. Chen, D.R. Yang, A. Lawrenz, H.J. Moeller, *J. Appl. Phys.* 97 (2000) 094909.
- [20] S.K. Bains, D.P. Griffiths, J.G. Wilkes, R.W. Series, K.G. Barraclough, *J. Electrochem. Soc.* 137 (1990) 647.
- [21] G.A. Rozgonyi, C.W. Pearce, *Appl. Phys. Lett.* 32 (1978) 747.
- [22] R. Falster, V.V. Voronkov, F. Quast, *Phys. Status. Solidi B* 222 (2000) 219.
- [23] M. Pagani, R.J. Falster, G.R. Fisher, G.C. Ferrero, M. Olmo, *Appl. Phys. Lett.* 70 (1997) 1572.
- [24] P. Török, L. Mule' stagno, *J. Microsc.* 188 (1997) 1.
- [25] G.R. Booker, Z. Laczik, P. Kidd, *Semicond. Sci. Technol.* 7 (1992) A110.
- [26] J. Xu, D.R. Yang, H.J. Moeller, *J. Appl. Phys.* 102 (2007) 114506.
- [27] S.A. Mchugo, C. Flink, *Appl. Phys. Lett.* 77 (2000) 3598.
- [28] T. Buonassisi, A.A. Istratov, S. Peters, C. Ballif, J. Isenberg, S. Riepe, W. Warta, R. Schindler, G. Willeke, Z. Cai, B. Lai, E.R. Weber, *Appl. Phys. Lett.* 87 (2005) 121918.
- [29] B. Mohadjeri, J.S. Williams, J. Wong-Leung, *Appl. Phys. Lett.* 66 (1995) 1889.
- [30] Peng Zhang, Hele. Vainola, Andrei A. Istratov, E.R. Weber, *Appl. Phys. Lett.* 83 (2003) 4324.
- [31] A. Bazzali, G. Borionetti, R. Orizio, D. Gambaro, R. Falster, *Mater. Sci. Eng. B* 36 (1996) 85.
- [32] Z.Q. Xi, D.R. Yang, J. Chen, J. Xu, Y.J. Ji, D.L. Que, H.J. Moeller, *Semicond. Sci. Technol.* 19 (2004) 299.
- [33] Z. Laczik, PhD Thesis, Scanning Infrared Microscope studies of inhomogeneities in Si and GaAs ingot materials, University of Oxford, 1992.
- [34] R.J. Falster, G.R. Fisher, G. Ferrero, *Appl. Phys. Lett.* 59 (1991) 809.
- [35] R. Falster, V.V. Voronkov, *Mater. Sci. Eng. B* 73 (2000) 87.
- [36] M. Seibt, K. Graff, *J. Appl. Phys.* 63 (1988) 4444.